Indian Journal of Chemistry
Vol. 63, August 2024, pp. 775-781
DOI: 10.56042/ijc.v63i8.8262

Synthesis and photoluminescent properties of Eu^{3+}, Dy^{3+}doped molybdate based novel $Ba_{0.5}Ca_{0.5}La_2(MoO_4)_4$ phosphors

Esra Öztürk*[a,c] & Murat Ebic[b]

[a] Karamanoğlu Mehmetbey University, Engineering Faculty,
Department of Materials Science and Engineering, Karaman, Turkey
[b] Karamanoğlu Mehmetbey University, Technical Sciences Vocational School,
Karaman, Turkey
[c] Hacettepe University, Faculty of Science, Department of Chemistry, Ankara, Turkey
E-mail: esracircir@gmail.com

Received 24 January 2024; accepted(revised) 30 July 2024

$Ba_{0.5}Ca_{0.5}La_{2-x-y}(MoO_4)_4$:x$Eu^{3+}$,y$Dy^{3+}$ with doping concentrations of xEu^{3+} and yDy^{3+} (x =0.01, 0.03, 0.05, 0.1 and y= 0.01) phosphors were synthesized by solid state reaction method, one of the high temperature solid state methods. The reactions were carried out in tube furnace at determined temperatures. Thermogravimetry-differential thermal analysis (TG/DTA) system was used to determine the synthesis temperature of the material and to examine its thermal behavior. The crystal structure of the material was checked with x-ray powder diffractometry (XRD), surface morphology and elemental analysis were done with scanning electron microscope (SEM). The photoluminescent properties of luminescence and excitation wavelength and luminescence duration were determined by photoluminescence spectrophotometer (PL). As a result of the analyses made with photoluminescence spectrophotometer, three emission bands were observed at 619 nm, 652 nm and 706 nm, resulting from the characteristic $^5D_0 \rightarrow {}^7Fj$ (J=2, 3 and 4) transitions of Eu^{3+} ions.

Keywords: Photoluminescence, XRD, Eu^{3+}, Molibdates

Inorganic luminescent materials have wide application with their wide composition options and unique physical and chemical properties[1-3]. However, these materials have been designed as multi-functional to obtain photocatalytic or piezoelectric properties as well as luminescence properties[4-8]. In addition, inorganic luminescent materials are indispensable for W-LED and opto-electronic applications. To date, W-LEDs are composed of INGaN (blue LED) and YAG:CE^{3+} (yellow-emitting) components and are widely used. However, perfection has not been reached yet regarding the red components used in such W-LEDs. Research continues on physicochemical stability for red-emitting W-LED components[9-11]. For this reason, there is a need for more research on red-emitting phosphors. At this point, Eu^{3+} comes to the fore with its unique red emission properties. Eu^{3+} ions in a host crystal commonly form the luminescent center by $^5D_0 \rightarrow {}^7F_J$ (J = 0, 1, 2, 3, 4) transitions. The $^5D_0 \rightarrow {}^7F_1$ transition is due to the magnetic dipole transition of $Eu^{3+}$and is observed around 590 nm. The red emission of Eu^{3+} at ~610 nm, which is also the focus of this study, is the $^5D_0 \rightarrow {}^7F_2$ transition resulting from the electric dipole transition. The relative emission intensities of the aforementioned transitions vary depending on whether the host crystal is doped with the center of inversion symmetry or not [9, 12-15].

$MLn_2(MoO_4)_4$ type crystal (M:M^{2+}, Ln: rare earth elements) has a *scheelite* structure. The first example of $MLn_2(MoO_4)_4$, (M:M^{2+}) type crystal structures is the $CaEu_2(MoO_4)_4$ crystal. Such crystal structures are formed as tetragonal units in space can be modeled in (3+2) dimensions. This structure consists of MoO_4 tetrahedrons and $(A)O_8$ square antiprisms. (A) position can be Ca^2+, Eu^{3+}, Yb^{3+}, Ho^{3+} ions or hole. In the MoO_4 tetrahedron, the molybdenum atom is surrounded by 4 oxygens in the center, while in the $(A)O_8$ square antiprism there is an atom such as Ca^{2+}, Eu^{3+}, Yb^{3+}, Ho^{3+} in the center and 8 oxygen atoms surrounding it[16]. Thanks to the similarity of the radii of the rare earth elements that can settle in the structure, these ions can be effectively doped into the crystal lattice. Naturally, materials with photoluminescent properties can be developed, as well as materials for the desired purpose. For this, impurity atoms can be doped into a crystal (host

crystal), these atoms are called "activator" atoms. These activator atoms are doped in very small amounts (1-10 mol%) to form a narrow energy band. They cause some differences in luminescence properties due to the formation of radiation and defect centers in the crystal they are added to. The most suitable doping atoms for this purpose are the rare earth elements, as they have partially filled 4f shells. The transitions between the partially filled 4f shells of the doping atoms, which are protected within the crystal field of the residential crystal and create additional energy levels, cause emission. Such luminescent materials in inorganic crystal structure in which the photoluminescent feature is observed are generally oxide, oxysulfide, sulfur, selenide, borate, phosphate, gallate, germanate, vanadate, sulfate, molybdate, aluminate, silicate and alumina silicate type compounds[17,18].

Until now, almost no research has been done on the doping of $MLn_2(MoO_4)_4$ crystal with rare earth elements and its photoluminescence properties. Also, there is no article about the $Ba_{0.5}Ca_{0.5}La_2(MoO_4)_4$ crystal and its photoluminescence properties. Therefore, in the present study, $Eu^{3+}$and Dy^{3+} doped $Ba_{0.5}Ca_{0.5}La_2(MoO_4)_4$ phosphors were synthesized for the first time. $Ba_{0.5}Ca_{0.5}La_{2-x-y}(MoO_4)_4$: xEu^{3+},yDy^{3+} phosphors with doping concentrations of xEu^{3+} and yDy^{3+} (x =0.01, 0.03, 0.05, 0.1 and y=0.01) phosphors were prepared by solid state reaction method. The synthesized phosphors were characterized by X-ray diffraction (XRD), thermogravimetry-differential thermal analysis (TG/DTA) system and scanning electron microscopy (SEM). The luminescence properties were investigated using photoluminescence (PL) photospectrophotometer.

Materials and Method

In this study, high temperature solid state method was used as the synthesis method. To form the $Ba_{0.5}Ca_{0.5}La_2(MoO_4)_4$:$xEu^{3+}$,$yDy^{3+}$ phosphors, the starting materials $BaCO_3$ (99.0%), $CaCO_3$(99.9%), La_2O_3(99.99%), MoO_3(99.9%), Eu_2O_3(99.99%), Dy_2O_3(99.99%) were weighed in stoichiometric ratios (x =0.01, 0.03, 0.05, 0.1 and y= 0.01) and ground in a gate mortar. In order to determine the reaction optimum of the prepared homogeneous starting materials mixture, the thermal behavior of samples were investigated with a heating rate of 10°C/min from room temperature to 1300°C by a Seiko Instruments Inc./Exstar TG/DTA 6200 system. According to the thermal analysis studies, the starting material mixture was preheated at 650°C for 10 hours and heat treated at 850°C for 10hours and slowly cooled down to room temperature. The crystal structure of the heat-treated samples was determined with the BRUKER AXS D8 ADVANCE model (40 kV, 30 mA, Cu-Kα, 0.02°/2θ) XRD. The surface morphology and EDX analyzes of the synthesized crystal systems were performed with a LEO 440 scanning electron microscope (SEM). Photo-luminescence properties were examined with a PTI Quanta Master 30 model photoluminescence spectrophotometer operating in the 200-900 nm range with a xenon lamp.

Results and Discussions

The thermal analysis result of the powder mixture of $Ba_{0.5}Ca_{0.5}La_2(MoO_4)_4$:0.01 Eu^{3+}consisting of starting materials $BaCO_3$, $CaCO_3$, La_2O_3, MoO_3 and Eu_2O_3 used in the synthesis of luminescent material is shown in the thermogram in the Fig. 1(a). According to the TG curve, a total mass loss of 5.0% occurs in four regions. The initial mass loss occurs at the rate of 0.5% in the temperature range of 260-354°C, and it reaches the maximum speed at 312°C. In the TG curve, it is seen that the second mass loss occurs at the rate of 2.3% in the temperature range of 374-570°C, it is consistent with the theoretical mass loss and reaches the maximum speed at 475°C in the DTG curve. These mass losses correspond to the mass loss of pure La_2O_3[19]. It is seen that the third and fourth mass losses in the TG curve occur at the rate of 2.2% in the temperature range of 570-772°C, and reach the maximum speed at 613 and 702°C in the DTG curve, which is compatible with the theoretical mass loss. These mass losses are due to the decomposition of $BaCO_3$ and loss of CO_2 and the mass loss of pure La_2O_3[19]. TG/DTA curves of $Ba_{0.5}Ca_{0.5}La_2(MoO_4)_4$: $0.01Eu^{3+}$,$0.01Dy^{3+}$, $Ba_{0.5}Ca_{0.5}La_2(MoO_4)_4$:$0.03Eu^{3+}$, $0.01Dy^{3+}$, $Ba_{0.5}Ca_{0.5}La_2(MoO_4)_4$:0.05 Eu^{3+},0.01 Dy^{3+}, $Ba_{0.5}Ca_{0.5}La_2(MoO_4)_4$:$0.1Eu^{3+}$,$0.01Dy^{3+}$ materials are also given in Fig. 1(b-e), respectively. The mass loss and the related temperatures for each sample are given in Table 1.

According to the DTA/TG curves, no mass change was observed after 770°C. Therefore, it was decided to apply a pre-heat treatment at 650°C for 10 hours in order to decompose $CaCO_3$ and $BaCO_3$ compounds into their oxides and CO_2. After pre-heating, a main heat treatment was applied at 850°C for 10 hours in the furnace in order to carry out the solid state reactions. X-Ray Powder Diffraction (XRD) analyzes were made in order to determine their crystal structures and unit cell parameters. The XRD

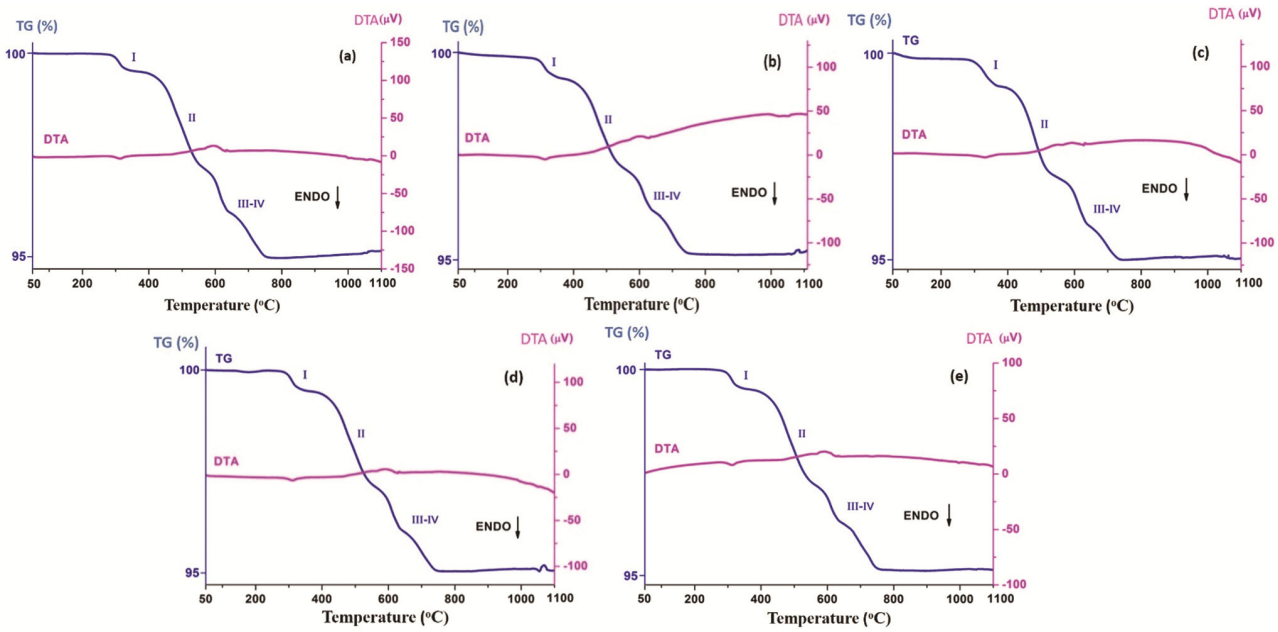

Fig. 1 — TG/DTA curves of (a)$Ba_{0.5}Ca_{0.5}La_2(MoO_4)_4$:0.01$Eu^{3+}$, (b) $Ba_{0.5}Ca_{0.5}La_2(MoO_4)_4$:0.01$Eu^{3+}$, 0.01$Dy^{3+}$, (c) $Ba_{0.5}Ca_{0.5}La_2(MoO_4)_4$:0.03$Eu^{3+}$, 0.01$Dy^{3+}$, (d) $Ba_{0.5}Ca_{0.5}La_2(MoO_4)_4$:0.05$Eu^{3+}$, 0.01$Dy^{3+}$, (e) $Ba_{0.5}Ca_{0.5}La_2(MoO_4)_4$:0.10$Eu^{3+}$, 0.01$Dy^{3+}$ phosphors

Table 1 — TG/DTA datas of $Ba_{0.5}Ca_{0.5}La_{2-x-y}(MoO_4)_4$:x$Eu^{3+}$,y$Dy^{3+}$ (x =0.01, 0.03, 0.05, 0.1 and y= 0.01) phosphors.

Phosphor	Total mass loss (%)	1. Mass loss(%)	2. Mass Loss (%)	3. and 4. Mass loss (%)
$Ba_{0.5}Ca_{0.5}La_2(MoO_4)_4$: 0.01$Eu^{3+}$	5	%0.5 (266°C -374°C) (Max. :312°C)	%2.3 (374°C -570°C) (Max. :475°C)	%2.2 (570°C -772°C) Max. (613-702°C)
$Ba_{0.5}Ca_{0.5}La_2(MoO_4)_4$: 0.01 Eu^{3+}, 0.01Dy^{3+}	5	%0.5 (260°C -354°C) (Max. :313°C)	%2.3 (354°C -558°C) (Max. :471°C)	%2.2 (558°C -769°C) Max. (611-701°C)
$Ba_{0.5}Ca_{0.5}La_2(MoO_4)_4$: 0.03 Eu^{3+} ,0.01Dy^{3+}	5	%0.5 (267 °C -360°C) (Max. :332°C)	%2.3 (360°C-548°C) (Max. :479°C)	%2.2 (548°C -747° C) Max. (612-700°C)
$Ba_{0.5}Ca_{0.5}La_2(MoO_4)_4$: 0.05 Eu^{3+},0.01 Dy^{3+}	5	%0.5 (257°C -354°C) (Max. :312°C)	%2.3 (354°C -565°C) (Max. :471°C)	%2.2 (565°C -761°C) Max. (610-699°C)
$Ba_{0.5}Ca_{0.5}La_2(MoO_4)_4$: 0.1 Eu^{3+},0.01 Dy^{3+}	5	%0.5 (258°C -361°C) (Max. :313°C)	%2.3 (361°C -565°C) (Max. :478°C)	%2.2 (565°C -767°C) Max. (633-681°C)

powder patterns of $Ba_{0.5}Ca_{0.5}La_2(MoO_4)_4$:0.01$Eu^{3+}$, $Ba_{0.5}Ca_{0.5}La_2(MoO_4)_4$:0.01$Eu^{3+}$,0.01$Dy^{3+}$, $Ba_{0.5}Ca_{0.5}La_2(MoO_4)_4$:0.03$Eu^{3+}$,0.01$Dy^{3+}$, $Ba_{0.5}Ca_{0.5}La_2(MoO_4)_4$: 0.05$Eu^{3+}$,0.01$Dy^{3+}$, $Ba_{0.5}Ca_{0.5}La_2(MoO_4)_4$:0.1$Eu^{3+}$,0.01$Dy^{3+}$ luminescent materials are given in Fig. 2 (a-e). The luminescent materials have single phase and their powder pattern compatible with the PDF card number JCPDS:00-035-0365. The unit cell parameters calculated for the monoclinic crystal systems were found as a=1079 pm, b=1061 pm, c=1277 pm, α=90°, β=90°, γ=90.44°, V=1461.89×10⁶ pm³.

After the applied heat treatment at 850°C for 12 hours, EDX and surface morphology analyzes of doped $Ba_{0.5}Ca_{0.5}La_2(MoO_4)_4$ luminescent materials

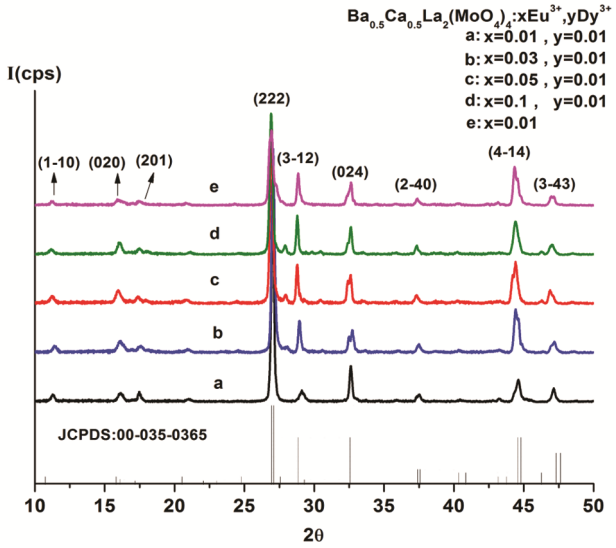

Fig. 2 — XRD patterns of $Ba_{0.5}Ca_{0.5}La_{2-x-y}(MoO_4)_4:xEu^{3+},yDy^{3+}$ (x =0.01, 0.03, 0.05, 0.1 and y= 0.01) phosphors at 850°C

were made by SEM and x20.000 times magnified images of the particles forming the materials were recorded. The SEM images of luminescent materials are shown Fig. 3 (a-e). Also, the EDX analyzes of luminescent materials are shown in the Fig. 4 (a-e) and the EDX analyzes data are listed in the Table 2. According to SEM images and EDX analysis, it is seen that there are no impurity elements in the structure, the particle sizes are around 0.1-4 μm and the particles are homogeneously dispersed.

The luminescence properties and life times of $Ba_{0.5}Ca_{0.5}La_2(MoO_4)_4:0.01Eu^{3+}$, $Ba_{0.5}Ca_{0.5}La_2(MoO_4)_4:0.01Eu^{3+},0.01Dy^{3+}$, $Ba_{0.5}Ca_{0.5}La_2(MoO_4)_4:0.03Eu^{3+},0.01Dy^{3+}$, $Ba_{0.5}Ca_{0.5}La_2(MoO_4)_4:0.05Eu^{3+},0.01Dy^{3+}$, $Ba_{0.5}Ca_{0.5}La_2(MoO_4)_4:0.1Eu^{3+},0.01Dy^{3+}$ luminescent materials were analyzed by photoluminescence spectrophotometer with wavelengths ranging from 200 nm to 900 nm. The effect of Eu^{3+}ions doped at different rates on the excitation and emission

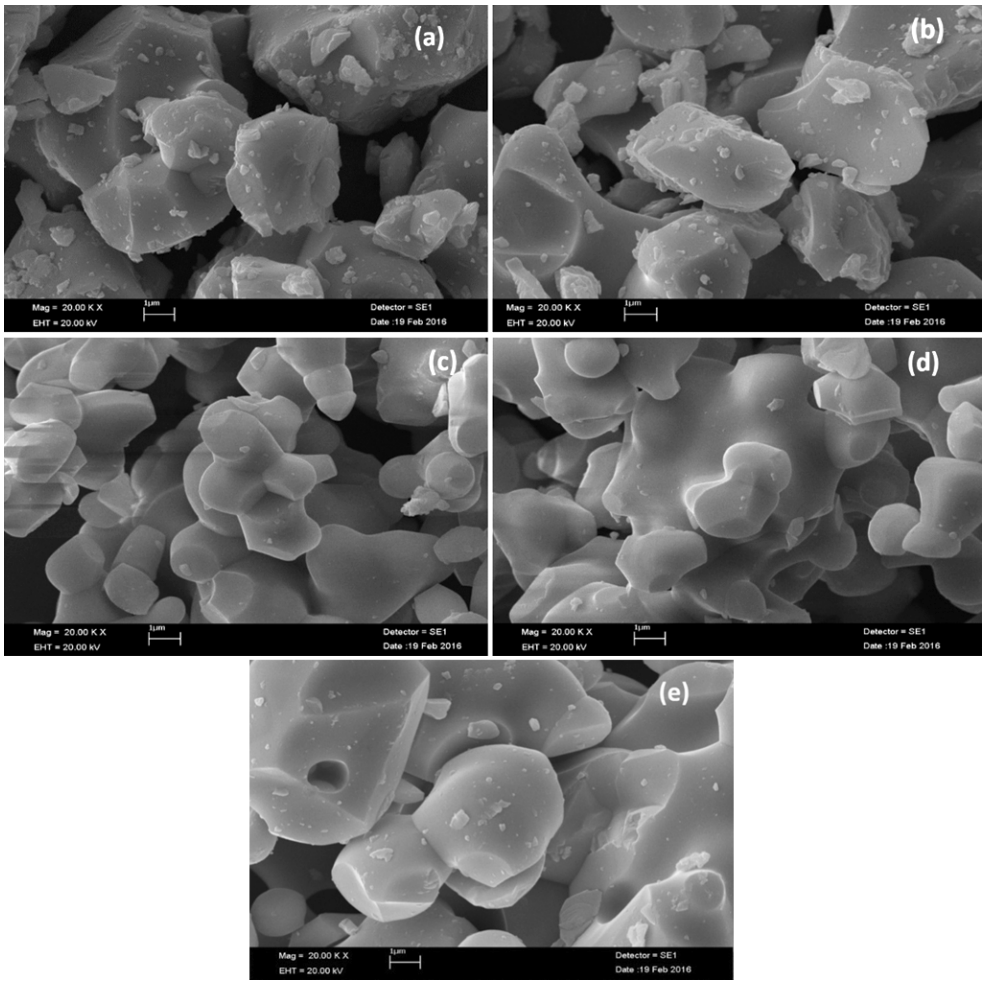

Fig. 3 — SEM images of (a) $Ba_{0.5}Ca_{0.5}La_2(MoO_4)_4:0.01Eu^{3+},0.01Dy^{3+}$, (b) $Ba_{0.5}Ca_{0.5}La_2(MoO_4)_4:0.03Eu^{3+},0.01Dy^{3+}$, (c) $Ba_{0.5}Ca_{0.5}La_2(MoO_4)_4:0.05Eu^{3+}$, $0.01Dy^{3+}$, (d) $Ba_{0.5}Ca_{0.5}La_2(MoO_4)_4:0.10Eu^{3+}$, $0.01Dy^{3+}$, (e) $Ba_{0.5}Ca_{0.5}La_2(MoO_4)_4:0.01Eu^{3+}$ phosphors

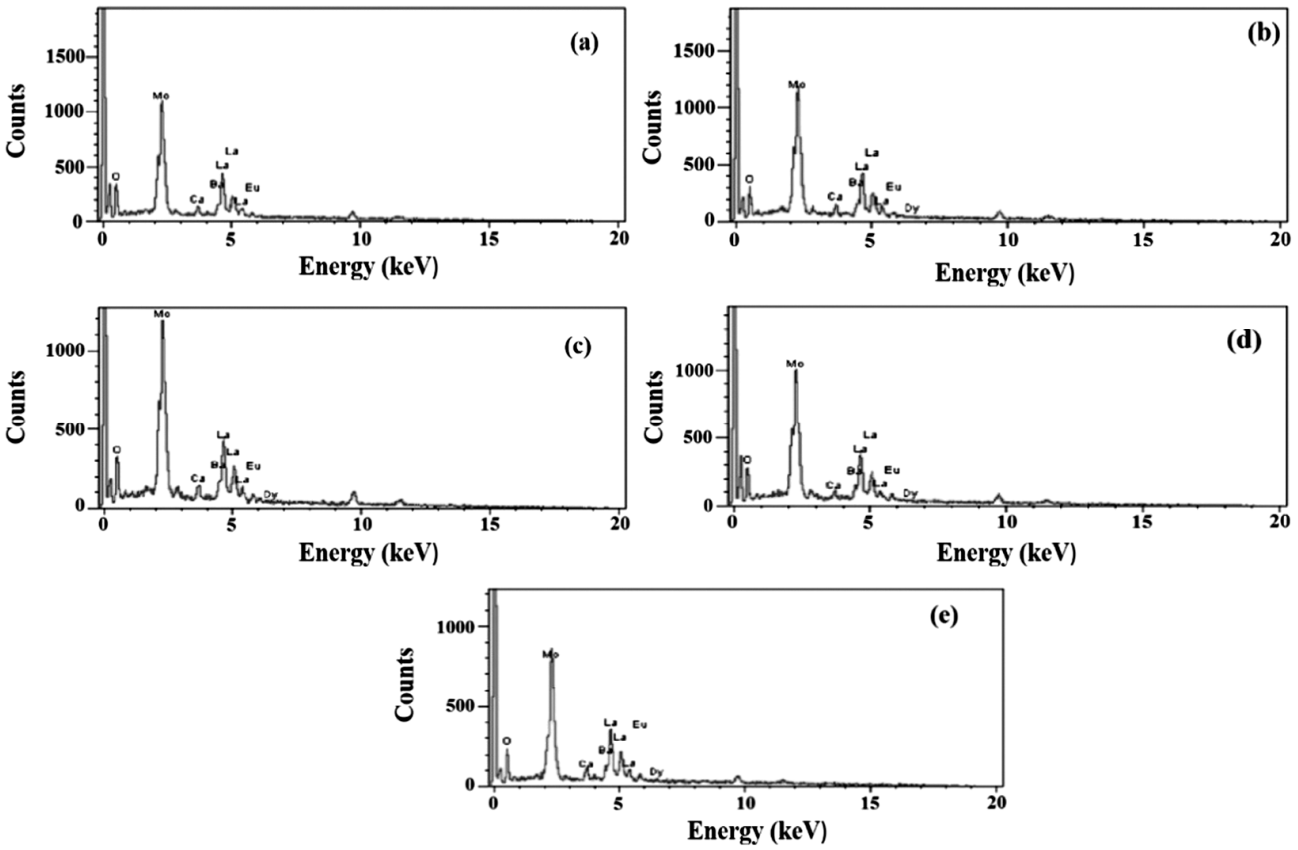

Fig. 4 — EDX analysis of (a)$Ba_{0.5}Ca_{0.5}La_2(MoO_4)_4$:0.01$Eu^{3+}$, (b) $Ba_{0.5}Ca_{0.5}La_2(MoO_4)_4$:0.01$Eu^{3+}$, 0.01$Dy^{3+}$, (c) $Ba_{0.5}Ca_{0.5}La_2(MoO_4)_4$:0.03$Eu^{3+}$, 0.01$Dy^{3+}$, (d) $Ba_{0.5}Ca_{0.5}La_2(MoO_4)_4$:0.05$Eu^{3+}$, 0.01$Dy^{3+}$, (e) $Ba_{0.5}Ca_{0.5}La_2(MoO_4)_4$:0.10$Eu^{3+}$, 0.01$Dy^{3+}$ phosphors

Table 2 — EDX data of $Ba_{0.5}Ca_{0.5}La_{2-x-y}(MoO_4)_4$:x$Eu^{3+}$,y$Dy^{3+}$ (x =0.01, 0.03, 0.05, 0.1 and y= 0.01) phosphors.

		Ba	Ca	La	Mo	O	Eu	Dy
$Ba_{0.5}Ca_{0.5}La_2(MoO_4)_4$:	Calculated %	6.80	1.99	27.52	38.02	25.36	0.15	0.16
0.01 Eu^{3+}, 0.01 Dy^{3+}	Experimental %	7.95	2.31	36.89	30.05	21.78	0.13	0.88
$Ba_{0.5}Ca_{0.5}La_2(MoO_4)_4$:	Calculated %	6.78	1.98	27.45	37.90	25.28	0.45	0.16
0.03 Eu^{3+}, 0.01 Dy^{3+}	Experimental %	9.43	2.16	38.07	27.89	21.70	0.34	0.41
$Ba_{0.5}Ca_{0.5}La_2(MoO_4)_4$:	Calculated %	6.76	1.97	27.40	37.72	25.24	0.75	0.16
0.05 Eu^{3+}, 0.01 Dy^{3+}	Experimental %	10.67	1.37	38.78	26.70	20.59	1.25	0.64
$Ba_{0.5}Ca_{0.5}La_2(MoO_4)_4$:	Calculated %	6.71	1.96	27.15	37.51	25.02	1.49	0.16
0.1 Eu^{3+}, 0.01 Dy^{3+}	Experimental %	8.47	0.99	33.53	31.76	22.84	1.88	0.53
$Ba_{0.5}Ca_{0.5}La_2(MoO_4)_4$:	Calculated %	6.81	1.99	27.57	38.08	25.40	0.15	-
0.01 Eu^{3+}	Experimental %	8.13	2.21	36.83	28.74	23.97	0.12	-

intensities of luminescent materials is shown in Fig. 5. As seen in the Fig. 5, all phosphors also exhibit the similar emission spectra and the characteristic luminescence bands of Dy^{3+} ions doped as co-activator were not observed. Two excitation bands of luminescent materials have been detected, resulting from the charge transfer of Eu^{3+}ions at 290 nm and $^7F_0 \rightarrow {}^5L_6$ transition of Eu^{3+}ions at 389 nm. The excitation peak at 389 nm ($^7F_0 \rightarrow {}^5L_6$), suggesting that the $Ba_{0.5}Ca_{0.5}La_{2-x-y}(MoO_4)_4$:x$Eu^{3+}$,y$Dy^{3+}$ with doping concentrations of xEu^{3+} and yDy^{3+} (x =0.01, 0.03, 0.05, 0.1 and y= 0.01) phosphors could be effectively excited by blue light and N-UV, having potential application in W-LED. As a result of these excitations, three emission bands were observed at 619 nm, 652 nm and 706 nm, resulting from the characteristic $^5D_0 \rightarrow {}^7Fj$ (J=2, 3 and 4) transitions of Eu^{3+} ions[20]. Among the three emission peaks, the strongest emission peak is the red emission peak at 619 nm. At the same time, no orange emission peak is

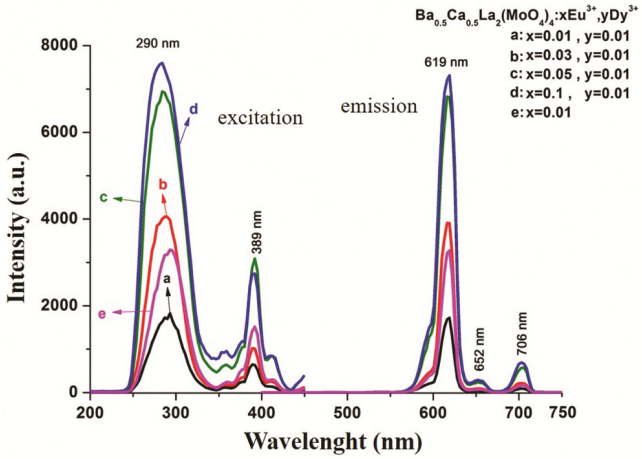

Fig. 5 — Photoluminescence spectra of $Ba_{0.5}Ca_{0.5}La_{2-x-y}(MoO_4)_4$: xEu^{3+},yDy^{3+} (x =0.01, 0.03, 0.05, 0.1 and y= 0.01) phosphors

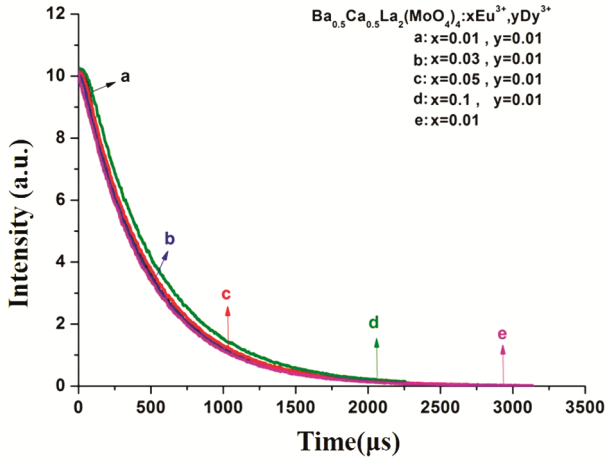

Fig. 6 — Lifetime spectra of $Ba_{0.5}Ca_{0.5}La_{2-x-y}(MoO_4)_4$: xEu^{3+},yDy^{3+} (x =0.01, 0.03, 0.05, 0.1 and y= 0.01) phosphors

observed. It indicates that Eu^{3+} ions locate the non-inversion symmetry site in the host crystal[9,21]. This condition leads to a dominant red emission by doping Eu^{3+} to the $Ba_{0.5}Ca_{0.5}La_{2-x-y}(MoO_4)_4$ host crystal, in accordance with the purpose of this study. As seen in the Fig. 5, the most intense red emission at 619 nm is obtained in $Ba_{0.5}Ca_{0.5}La_2(MoO_4)_4$:$0.1Eu^{3+}$,$0.01Dy^{3+}$ composition. Thus we can say that the optimum doping ratios for $Ba_{0.5}Ca_{0.5}La_{2-x-y}(MoO_4)_4$ host crystal are x=$0.1Eu^{3+}$, and y=$0.01Dy^{3+}$. Further increase of doping concentration leads to luminescence intensity decline due to concentration quenching.

The decay time graphs of the luminescent materials are given in the Fig. 6 and the decay times of the material was calculated using below equation and are shown in the Table 3.

Table 3 — Decay times of $Ba_{0.5}Ca_{0.5}La_{2-x-y}(MoO_4)_4$:$xEu^{3+}$,$yDy^{3+}$ (x =0.01, 0.03, 0.05, 0.1 and y= 0.01) phosphors.

Phosphor	Activator ion and doping rate (mole)	Co-Activator ion and doping rate (mole)	Decay time (τ_1)
$Ba_{0.5}Ca_{0.5}La_2(MoO_4)_4$	0.01 Eu^{3+}	0.01 Dy^{3+}	442.2 µs
	0.03 Eu^{3+}	0.01 Dy^{3+}	453.3 µs
	0.05 Eu^{3+}	0.01 Dy^{3+}	43.35 µs
	0.10Eu^{3+}	0.01 Dy^{3+}	62.35 µs
	0.01 Eu^{3+}	-	423.6 µs

$I = A_1\exp(-t/\tau_1) + C_1$.

I : luminescence intensity, A_1, C: constant, t: time and τ_1 : decay time.

It can be clearly seen from Table 3 that the composition with the longest decay time is $Ba_{0.5}Ca_{0.5}La_2(MoO_4)_4$:$0.03Eu^{3+}$,$0.01Dy^{3+}$.

Conclusions

In this study, $Ba_{0.5}Ca_{0.5}La_{1.99}Eu_{0.01}(MoO_4)$, $Ba_{0.5}Ca_{0.5}La_{1.98}Eu_{0.01}Dy_{0.01}(MoO_4)_4$, $Ba_{0.5}Ca_{0.5}La_{1.96}Eu_{0.03}Dy_{0.01}(MoO_4)_4$, $Ba_{0.5}Ca_{0.5}La_{1.94}Eu_{0.05}Dy_{0.01}(MoO_4)_4$, $Ba_{0.5}Ca_{0.5}La_{1.89}Eu_{0.10}Dy_{0.01}(MoO_4)_4$ luminescent materials were firstly synthesized by high temperature solid state reaction methods. It was determined that all the materials have single-phase monoclinic crystal system according to XRD data. As a result of the analyses made with photoluminescence spectro-photometer, three emission bands were observed at 619 nm, 652 nm and 706 nm, resulting from the characteristic $^5D_0 \rightarrow {}^7Fj$ (J=2, 3 and 4) transitions ofEu^{3+} ions. Since Eu^{3+} ions locate the non-inversion symmetry site in the $Ba_{0.5}Ca_{0.5}La_2(MoO_4)_4$ host crystal, desired dominant red emission is obtained at 619 nm. Also, all phosphors could be effectively excited by blue light and NUV (389 nm). For these reasons, all phosphors have significant potential for WLEDs applications. As it is known, materials with red emission are very important for opto-electronic applications. According to the photoluminescent results obtained in this study, all the luminescent materials synthesized are good candidates for opto-electronic applications with red components.

Acknowledgements

The authors would like to thank to the Karamanoglu Mehmetbey University's, Scientific Research Projects Commission (BAP), under the Project Number: 03-YL-15, Republic of Turkey, for its financial support.

References

1 Uzun E, Öztürk E, Ozpozan N K, *Luminescence*, 33 (2018) 1346.

2 Öztürk E & Ozpozan N K, *JThermal Anal Calor*, 117 (2014)573-578.
3 Öztürk E, Ozpozan N K & Uzun E, *J Chinese Chem Soc*, 62 (2015) 47.
4 Özlü H, Kırkgeçit R, Öztürk E & Kılıç D F, *J Photochem & Photobio*, 418 (2021) 113338.
5 Kırkgeçit R, Özlü H, Kılıç Dokan F. and Öztürk E, *J Photochem & Photobio*, 423 (2022) 113602.
6 Kırkgeçit R, Özlü H, Kılıç Dokan F & Öztürk E, *J Rare Earths*, 40 (2022) 1619.
7 Öztürk E & Sarılmaz E, *Mat Chem Phy*, 239 (2020) 122085.
8 Öztürk E & Sarılmaz E, *Mat Res Exp*, 6 (2019) 105710.
9 Wu Z, Ai S, Chen H, Zhou T, Liu M, Zhao Y, Xin Lai, Jian Bi & Daojiang G, *Optics & Laser Tech*, 150 (2022) 107947.
10 Parauha Y R, Yadav R S & Dhoble S J, *Opt Laser Tech*, 124 (2020) 105974
11 Pasiński D & Sokolnicki J, *J Alloys Comp*, 695 (2017) 1160.
12 Slimi S, Loiko P, Volokitina A, Bogdanov K, Solé R M, Aguiló M, Díaz F, Salem E B & Mateos X**,** *J Lumin*, 241 (2022) 118523.
13 Macedo W C, Bispo A G J, Rocha K D O, Albas A E D S, Pires A M, Teixeira S R & Longo E, *Today Comm*, 24 (2020) 100966
14 Mofokeng S J, Noto L L & Dhlamini M S, *J Lumin*, 228 (2020) 117569
15 Balakrishna A, Reddy L, Ntwaeaborwa O M & Swart H C, *J Mol Struc*, 1203 (2020) 127375.
16 Abakumov A M, Morozov V A, Tsirkin A A, Verbeek J V & Hadermann J, *Inorg Chem,* 53 (2014) 9407.
17 Yuan S, Wang L, Yang Y, Cheviré F, Tessier F & Chen G, *Ceramics Int*, 42 (2016) 12508.
18 Öztürk E, Ozpozan K N & Uzun E, *J Chinese Chem Soc,* 2016, 63 (2016) 213.
19 Bernal S, Botana F J, Garcia R & Rodriguez-Izquierdo J M, *Thermochimica Acta*, 66 (1983) 139.
20 Jinsheng L, Dan Z, Bin Y, Ruiqing L, Qian Z & Quanhui V Z, *J Luminescence*, 134 (2013) 533.
21 Wei B, Liu Z, Xie C, Yang S, Tang W, Gu A, Wong W T & Wong K L, *J Mater Chem*, 3 (2015) 12322.